ARTICLE

Correlations between Synaptic Initiation and Meiotic Recombination: A Study of Humans and Mice

Jennifer R. Gruhn,[1] Nasser Al-Asmar,[2] Rachael Fasnacht,[1] Heather Maylor-Hagen,[1] Vanessa Peinado,[3] Carmen Rubio,[3] Karl W. Broman,[4] Patricia A. Hunt,[1] and Terry Hassold[1,*]

Meiotic recombination is initiated by programmed double strand breaks (DSBs), only a small subset of which are resolved into crossovers (COs). The mechanism determining the location of these COs is not well understood. Studies in plants, fungi, and insects indicate that the same genomic regions are involved in synaptic initiation and COs, suggesting that early homolog alignment is correlated with the eventual resolution of DSBs as COs. It is generally assumed that this relationship extends to mammals, but little effort has been made to test this idea. Accordingly, we conducted an analysis of synaptic initiation sites (SISs) and COs in human and mouse spermatocytes and oocytes. In contrast to our expectation, we observed remarkable sex- and species-specific differences, including pronounced differences between human males and females in both the number and chromosomal location of SISs. Further, the combined data from our studies in mice and humans suggest that the relationship between SISs and COs in mammals is a complex one that is not dictated by the sites of synaptic initiation as reported in other organisms, although it is clearly influenced by them.

Introduction

Aneuploidy is the most common category of human chromosome abnormality and is the leading genetic cause of spontaneous abortions and congenital birth defects.[1] The mechanisms that give rise to aneuploidy remain obscure, but it is clear that abnormalities in meiotic recombination are an important contributor. Specifically, studies of human trisomies indicate that failure to recombine or recombination events that occur too close to, or too far from, the centromere are important risk factors for nondisjunction at the first meiotic division.[1] The correlation is particularly strong for human female meiosis; e.g., the majority of cases of maternally derived trisomy 21 (Down syndrome [MIM: 190685]) have been linked to absence of recombination or to proximally or distally placed crossovers.[2–4]

We and others[5–7] have been interested in determining the basis of recombination abnormalities in the human female and, more generally, in elucidating the factors that control the levels and placement of recombination events in mammals. Presumably, such factors can act in one of two ways—either by affecting the number or location of meiotic double-strand breaks (DSBs) or by affecting the likelihood that DSB intermediates are resolved as crossovers (COs). Recently, Kong et al.[8] presented evidence for the latter, linking sequence variants for loci encoding proteins that act downstream of DSBs (e.g., *MSH4* [MIM: 602105], *RNF212* [MIM: 612041]) to variation in genome-wide recombination rates in humans. However, there is also ample evidence that events acting at or before the time of DSB formation influence the number of crossovers. For example, in cytological studies of meiotic prophase in male mice, we observed a direct correlation between the number of foci of the DSB-associated protein RAD51 in early zygotene and the CO-associated protein MLH1 in pachytene; i.e., strains of mice with higher RAD51 levels had higher MLH1 values.[9] Similarly, in studies of human males and females, we found proportional increases in the numbers of both RAD51 and MLH1 foci in females, with female:male ratios of approximately 1.4 and 1.9, respectively.[6] This suggests that the well-known excess of crossovers in human females might be attributable to sex-specific differences in chromatin dynamics at the onset of meiosis.[10–15]

The nature of any such sex-specific difference is unclear, but male-female variation in the way in which the synaptonemal complex (SC) is assembled is an attractive candidate. The SC is the meiosis-specific lattice structure that "zippers" homologs together to bring homologous sequences into close proximity. The basics of SC formation are conserved throughout evolution, but there are notable sex-specific differences in SC morphology and in the way in which the mature SC is generated. For example, the SC is longer in females than males in a number of species (reviewed in Kleckner et al.[16]) and, in preliminary studies of human meiosis, we observed remarkable differences between males and females in the location of synaptic initiation sites (SISs).[6] This observation is notable, given the reported association between sites of synapsis and COs in some species (reviewed in Henderson and Keeney[17] and Zickler et al.[18]).

To determine whether the relationship between synaptic initiation sites and crossovers applies to mammalian species, we combined immunofluorescence (IF) and

[1]School of Molecular Biosciences and Center for Reproductive Biology, Washington State University, Pullman, WA 99164, USA; [2]Preimplantation Genetic Diagnosis Unit, Igenomix, Miami, FL 33126, USA; [3]Preimplantation Genetic Diagnosis Unit, Igenomix, Paterna, Valencia 46980, Spain; [4]Department of Biostatistics and Medical Informatics, University of Wisconsin-Madison, Madison, WI 53706, USA
*Correspondence: terryhassold@vetmed.wsu.edu
http://dx.doi.org/10.1016/j.ajhg.2015.11.019.

Table 1. Human Study Population

ID Number	Age[a]	No. of Zygotene Cells	MLH1 Analysis	
			No. of Pachytene Cells	Mean MLH1 ± SE
Male				
OA32	63	62	69	48.3 ± 0.6
OA34	41	50	63	48.7 ± 0.5
OA36	38	52	64	46.1 ± 0.3
Female[b]				
SF105	19/5	66	44	59.6 ± 1.5
SF150	19/4	95	44	69.4 ± 1.5
SF186	23/4	58	73	77.1 ± 1.4
SF320	19/5	36	27	70.0 ± 1.4
SF333	17/5	28	43	69.2 ± 1.6

[a]Age in years for males; in weeks/days of gestation for females.
[b]Each of the five fetal ovarian samples was analyzed for the global MLH1 foci per cell and chromosome-specific synaptic initiation sites on chromosomes 1 and 16. However, MLH1 foci on chromosome 1 were gathered only from SF105, SF320, and SF333. Additionally, only SF105, SF150, and SF186 were analyzed for chromosome 21 SISs and MLH1 foci.

fluorescence in situ hybridization (FISH) to identify the locations of SISs and CO-associated proteins during meiotic prophase in oocytes and spermatocytes from humans and mice. Our observations indicate surprising sex- and species-specific differences in synapsis, including variation in both the number and chromosomal locations of SISs. Further, although we were unable to confirm a direct 1:1 correspondence between SISs and COs, our results suggest that a subset of crossovers are linked to sites of synaptic initiation in both species and in both sexes.

Material and Methods

Ethics Statement

This study was conducted according to the principles expressed in the Declaration of Helsinki. All procedures were reviewed and approved by the Instituto Valenciano de Infertilidad, University of California, San Francisco and Washington State University Institutional Review Boards, and written informed consent was obtained from all study participants.

All animal experiments were approved by the WSU institutional Animal Care and Use Committee, which is fully accredited by the American Association for Accreditation of Laboratory Animal Care.

Sample Populations

The human sample population consisted of three testicular biopsies (OA32, OA34, and OA36) and five fetal ovaries (SF105, SF150, SF186, SF320, and SF333). Testicular biopsies were obtained from patients being seen for infertility at the Instituto Valenciano de Infertilidad (IVI), Valencia, Spain. Analyses of infertile patients were restricted to individuals diagnosed with obstructive azoospermia, attributable to a previous vasectomy. Fetal ovaries were obtained from elective terminations of pregnancy performed at the San Francisco General Hospital Women's Options Center in San Francisco, California. Detailed patient information for both human male and female samples is found in Table 1.

Wild-type male and female C57BL/6J mice from The Jackson Laboratory were used in this study. Animals were housed in ventilated rack caging in a pathogen-free facility. Four adult males from four different litters were analyzed at >8 weeks and were processed for analysis of SISs in zygotene cells and MLH1 foci in pachytene cells. Analysis of SISs in oocytes was based on seven embryonic day 16 (E16) females from four litters, and MLH1 studies on six E18.5 females from three litters.

Tissue Processing

For human tissue, material was collected from testicular or fetal ovarian tissues and processed via a standard surface-spreading technique.[19] For testicular biopsies, tissue was macerated and incubated in hypotonic solution for approximately 1 hr, and immunostaining was performed within 24 hr of slide preparation as previously described.[20] For females, fetal ovaries were isolated, excess connective tissue was removed, and the ovaries were placed in a hypoextraction buffer and subsequently macerated and spread onto microscope slides for immunostaining the following day.[5]

For mouse tissue, preparations were made via a standard surface-spreading technique.[19] Slides were air-dried, washed in 0.4% Photo-flo to remove debris, and immediately stained.

Immunostaining

Slides from Human Tissue

Slides from human testicular or ovarian tissues were immunostained via similar methodology to that of Cheng et al.[5] Antibodies were diluted in sterile filtered 1× ADB consisting of 10 ml normal donkey serum (Jackson ImmunoResearch), 3 g BSA (Sigma-Aldrich), 50 μl Triton X-100 (Alfa Aesar), and 990 ml PBS. Incubations were performed in a dark humid chamber at 37°C.

Slides were first blocked in 1× ADB for 1 hr, then incubated overnight in a 37°C humid chamber with CREST (Fisher; human CREST antiserum; 1:500) and MLH1 (BC PharMingen; mouse anti-human; 1:75). SYCP3 (Novus; rabbit anti-human; 1:150) was added and slides incubated for 2 hr, followed by 30 and 60 min washes in 1× ADB. Secondary antibodies (Jackson

ImmunoResearch) were added for overnight incubation; i.e., FDAM (fluorescein anti-mouse; 1:75) and ADAH (AMCA anti-human; 1:100), followed by a 45 min incubation with RDAR (rhodamine anti-rabbit; 1:100) and two final washes in 1× PBS for 30 min and 60 min. Slides were fixed with Prolong Gold Antifade reagent (Invitrogen), sealed with rubber cement, and stored at 4°C until analysis.

Immunostaining for simultaneous visualization of SYCP1 and SYCP3 followed a slightly modified protocol. After blocking in 1× ADB, slides were incubated overnight with CREST (Fisher; human CREST antiserum; 1:500) and SYCP1 (Santa Cruz; goat anti-human; 1:150). Slides were pre-washed in 1× ADB for 30 min and 60 min, followed by a 2 hr incubation with SYCP3 (Novus; rabbit anti-human; 1:150). Slides were washed in 1× ADB for 30 min and 60 min, then incubated for 2 hr with secondary antibodies rhodamine anti-goat (RDAG; 1:150) and AMCA anti-human (ADAH; 1:100) (Jackson ImmunoResearch), followed by 30 and 60 min washes in 1× PBS. Slides were then incubated with secondary antibody fluorescein anti-rabbit (FDAR; Jackson ImmunoResearch) diluted 1:100 for 45 min, washed in 1× PBS for 45 min, and washed in 1× PBS overnight. Slides were fixed with Antifade (Invitrogen), sealed with rubber cement, and stored at 4°C.

Slides from Mouse Tissue

Slides from mouse testicular or ovarian tissue were stained with a slightly modified protocol. After blocking for 1 hr in 1× ADB, slides were incubated with MLH1 (Calbiochem; rabbit anti-mouse; 1:60) or SYCP1 (Novus Biologicals; rabbit anti-mouse; 1:100) overnight at 37°C. SYCP3 (Santa Cruz Biotechnology; mouse anti-mouse) diluted 1:500 was added after a brief wash in 1× ADB, incubated for 2 hr, followed with a 5–7 hr 1× ADB wash, and then incubated overnight with Alexa Fluor 488-conjugated AffiniPure Donkey Anti-Rabbit (AFDAR; Jackson Immunoresearch Laboratories; 1:60) at 37°C. Less than 12 hr later, the slides were briefly washed in 1× ADB and Cy3-conjugated AffiniPure Donkey Anti-mouse (CDAM; Jackson Immunoresearch Laboratories; 1:1,000) was added and incubated for 45 min. Incubation was then followed with 30 and 60 min 1× PBS washes. 20 μl Prolong Gold Antifade with DAPI (Invitrogen) was added to the slides and a coverslip applied. All slides were imaged on a Zeiss epifluorecence microscope with coordinates noted for each cell for subsequent fluorescence in situ hybridization (FISH) analysis.

Fluorescence In Situ Hybridization

Human male samples were hybridized with subtelomeric 1p and 16p FISH point probes (Cytocell Aquarius LPT01PR-A and LPT16PG-A). Human female samples were hybridized with FISH whole chromosome paint probes to chromosomes 1, 16, and 21 (Cytocell Aquarius LPP01R-A, LPP01G-A, LPP16G-A, and LPP21R-A). Stained slides were washed in 2× SSC for 2 min and dehydrated in ethanol washes (70%, 85%, 100%) for 2 min each, and 20 μl probe was placed on each slide. Coverslips were added, sealed with rubber cement, and denatured for 2 min on a 75°C hotplate. Slides were incubated at 37°C overnight, washed in 0.4× SSC at 72°C for 2 min, drained and washed in 2× SSC/0.05% Tween20 at room temperature for 30 s, and drained. Prolong Gold Antifade reagent with DAPI (Invitrogen) was then applied, and the slides stored at 4°C. Cells that had been previously identified for SIS or MLH1 immunostaining were re-located and the FISH images captured.

Mouse samples were hybridized with FISH whole chromosome paint probes to chromosomes 1, 11, and 19 (Applied Spectral Imaging) using the manufacturer's instructions. Slides were denatured in a 72°C 70% fomamide/2× SSC bath for 1 min, followed by a dehydration series of ice-cold 70% ethanol and room temperature 70%, 80%, and 100% ethanol for 2 min each, and air-dried. 3.5 μl of each probe was heated for 7 min in an 80°C thermocycler. Probe was added to the dried slide, sealed with a heated coverslip, and incubated overnight in a 37°C humid chamber.

Cytological Analysis of SISs and MLH1

For both species and both sexes, the locations of SISs and MLH1 foci were determined with MicroMeasure 3.3;[21] for chromosome 1 in humans, we arbitrarily took the longest arm on MicroMeasure to be 1q. Sites of synaptic initiation were determined by the presence of merged SYCP3 signals (human males) or the presence of short SYCP1 fragments (human females and mouse males and females) in zygotene-stage cells. In general, we restricted our analyses to SISs with merged SYCP3 signals or SYPC1 signals that comprised less than 25% of the length of the SC.

Pachytene-stage cells were analyzed for the number and location of MLH1 foci. A focus was counted only if the MLH1 signal co-localized with SYCP3, was punctate in appearance, and was separated from adjacent MLH1 foci by at least one signal domain. All cells were scored by at least two observers. MLH1 locations were determined as the distance (in microns) from the centromere to the MLH1 focus along the SC. This distance was then converted to a percentage of the SC length, to take into account SC length variation.

Results

In previous studies of synapsis, we analyzed zygotene-stage spermatocytes from six human males and determined the number and distribution of synaptic initiation sites.[22] We defined synaptic initiation sites (SISs) as the union of homologous axial elements, as detected by merged signals of the axial element protein SYCP3 or by the presence of the transverse filament protein SYCP1. These studies suggested that, with the exception of the short arms of acrocentric chromosomes, SISs are found at the distal tip of each chromosome arm; synapsis "zippers" inward from the distal SISs toward the centromere; and the centromere acts as a barrier to synapsis, and is typically the last region to fully synapse.[22] However, a number of important questions remain. (1) Is the pattern of synapsis the same in human males and females? (2) How does human synapsis compare to other mammalian species? (3) In mammals, do some, or all, SISs localize to future sites of crossing-over? To address these questions, we initiated studies to examine sex- and species-specific differences in synapsis.

Synapsis in Human Males and Females

We examined 164 zygotene-stage spermatocytes from three obstructive azoospermic males (Figure 1; Table 1), focusing on two chromosomes, a large metacentric (chromosome 1) and a small metacentric (chromosome 16). We first determined the number of SISs per chromosome

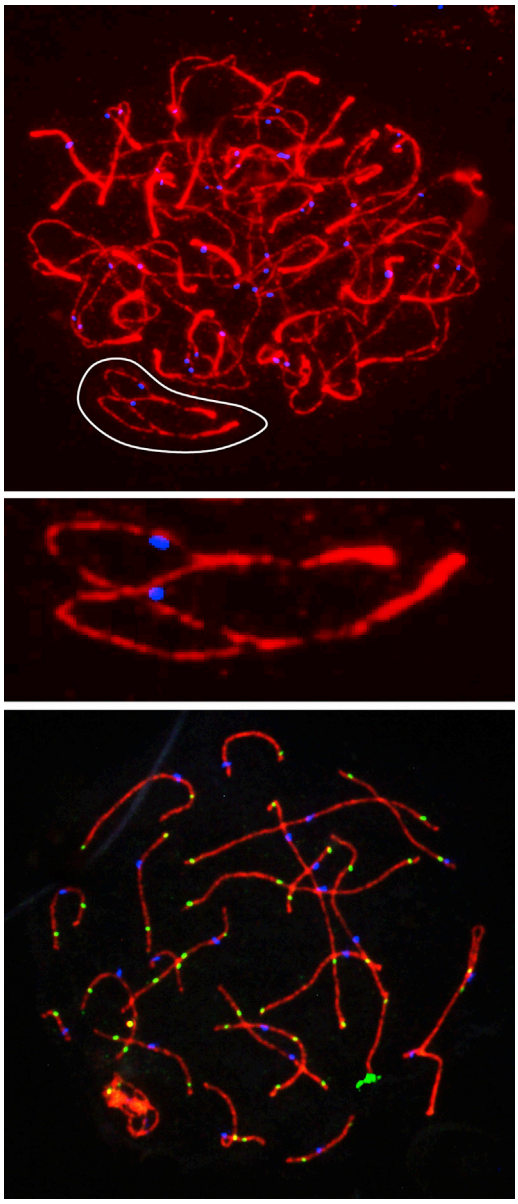

Figure 1. Synapsis Initiates near the Chromosome Ends in Human Males

Top: Image of a zygotene-stage spermatocyte, immunostained for the axial element protein SYCP3 (red) and centromere-associated CREST (blue). Synapsed chromosome regions are evident as intense, merged SYCP3 signals.

Middle: Enlargement of the circled partially synapsed chromosome pair from the above image, showing merged SYCP3 signals at the chromosome ends but not at the centromere.

Bottom: Use of a region-specific FISH probe (in this instance, to a locus on distal 1p; in green) to identify individual chromosomes in prophase-stage cells; in this case, the imaged spermatocyte is at pachytene.

and found little difference between the two chromosomes. That is, despite their large difference in size, each almost always exhibited one SIS per chromosome arm, or a total of two per chromosome (mean SISs ± SE per chromosome were 1.96 ± 0.02 for chromosome 1 and 1.98 ± 0.02 for chromosome 16), and more than two SISs were never observed for either chromosome (Figure 2A; Table 2). On initial inspection it appeared that the length of the SIS on one arm was similar to that on the other arm. This prompted us to test for the correlation between the lengths (in microns) of the p- and q-arm SIS tracts on individual chromosomes. We found a strong correlation between the lengths of p- and q-arm SISs on chromosome 1 (Pearson's correlation = 0.36, $p < 0.0001$; Figure S1), but not on chromosome 16 (data not shown).

Because no major differences were evident among the three individuals analyzed (Figure 2A), we pooled the data and mapped the SIS locations (Figure 2B). For this analysis, we were interested in examining the earliest stages of synapsis; accordingly, we restricted our analysis to chromosomes on which the SIS comprised less than 25% of the total SC length. Each chromosome arm was subdivided into five equal segments—centromeric, proximal, interstitial, distal, and telomeric—and the proportion of SISs localizing to each segment was tallied (Figure 2B). For these analyses (and for subsequent studies of SISs in human females and in mice), we took the mid-point of the merged SYCP3 tract or the SYCP1 tract as the location of the SIS. For both chromosomes 1 and 16, more than one-half of all SISs fell in the telomeric regions (i.e., 63.7% for chromosome 1 and 59.0% for chromosome 16) and almost all of the remaining SISs were located in the distal regions. Thus, in virtually all instances, we observed two SISs per chromosome, one near the end of the short arm and one near the end of the long arm. The patterns were consistent with our previous findings[22] and indicate a single strategy to synapsis in human males.

We conducted comparable studies of zygotene-stage human oocytes. In addition to analyses of chromosomes 1 and 16, for three of the five ovarian samples we examined the small acrocentric chromosome 21 because of its clinical relevance. In total, we analyzed the number and location of SISs in 283 zygotene oocytes (see Table 1). Representative images are provided in Figure 3, and summaries of the results are given in Figure 4, Table 2, and Figure S2. No obvious differences were evident among individuals in the number of SISs on chromosomes 16 and 21 and the locations of the SISs were similar for all individuals on all three chromosomes. However, we observed among-individual variation in the number of SISs on chromosome 1 ($\chi^2 = 62.37$; $p < 0.005$) and at least for chromosome 16, two of five individuals (SF320 and SF333) appeared to have somewhat different distributions of SISs, even if the differences did not reach statistical significance. Clearly, additional analyses of more fetal ovarian samples—and more chromosomes—will be useful in determining the extent of among-individual variation in SIS patterns.

Importantly, there were several obvious differences between the SIS patterns of females and males. Unlike males, the number of SISs per chromosome was highly variable in females: i.e., from 1 to 12 for chromosome 1 (mean = 5.71 ± 0.22), from 1 to 6 for chromosome 16

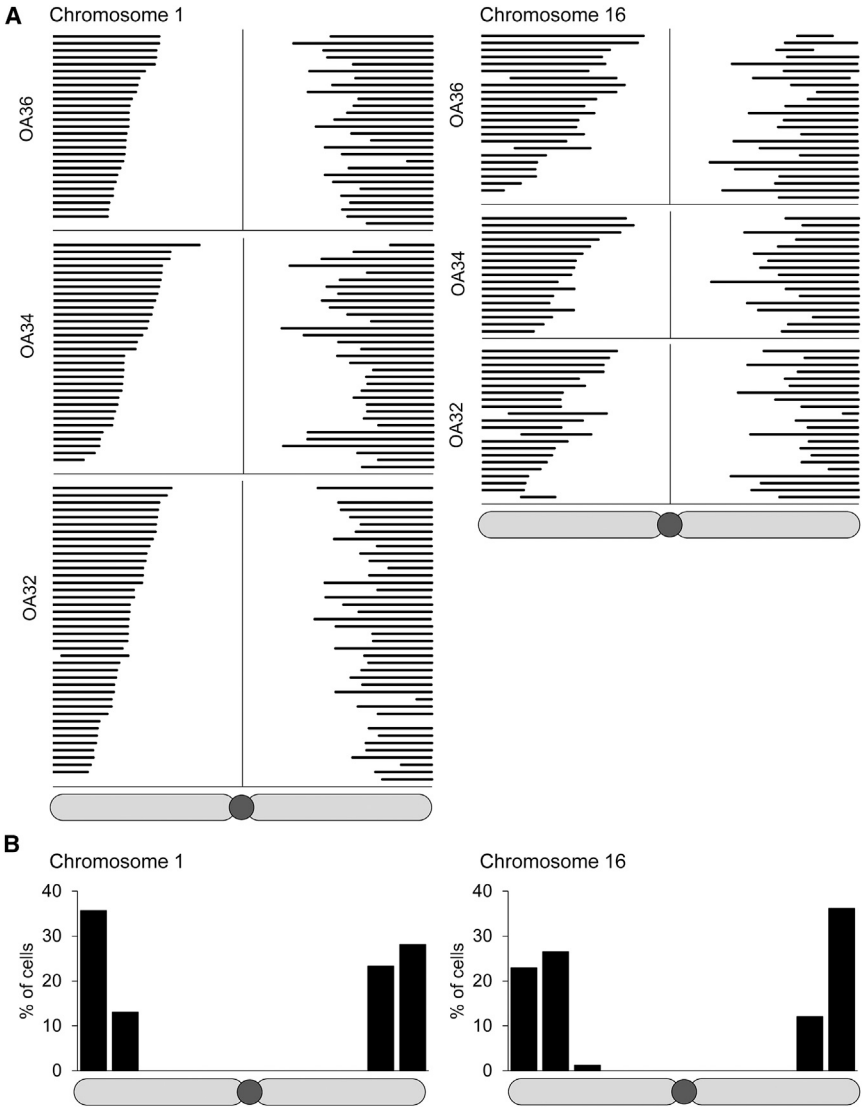

Figure 2. Chromosomal Locations of SISs in Human Males

(A) Chromosomal locations of SISs on individual chromosomes 1 or 16 from three testicular samples (OA32, OA34, and OA36). Each row shows the approximate length and location (as a percent of SC length) of SIS tracts on partially synapsed homologs; in total, we examined 102 partially synapsed chromosomes 1 and 63 partially synapsed chromosomes 16.

(B) A subset of data (SISs with lengths less than 25% of the chromosome length) from the three samples, showing the proportion of SISs in each of the different chromosome regions (i.e., centromeric, proximal, interstitial, distal, or telomeric) on the short and long arms of chromosomes 1 and 16. For this analysis, the location of an SIS was taken as the midpoint of the merged SYCP3 signal.

(mean = 2.35 ± 0.07) (Figure 2B), and from 1 to 4 for chromosome 21 (mean = 1.70 ± 0.06) (Table 3; Figure S2). However, as in the male, there was a correlation between SIS lengths on the p and q arms of chromosome 1 (Pearson's correlation = 0.70; $p < 0.0005$; Figure S1), although the number of observations was limited and a similar correlation was not evident on chromosome 16 or 21 (data not shown).

Strikingly, pericentromeric SISs, which were never seen in males, were common in females. Representative zygotene images showing SISs at or near the centromere are provided in Figure 3. Indeed, we occasionally identified cells in which the meiotic bouquet was preserved, demonstrating the presence of pericentromeric SISs in cells at early stages of synapsis (e.g., Figure S3).

The presence of pericentromeric SISs appeared to be a feature of all chromosomes, including the three on which we focused (i.e., 1, 16, and 21), with the majority of SCs containing an SIS that abutted or spanned the centromere (Figures 4A and S2A). Further, two separate analyses of the data provide evidence that pericentromeric sites are among the first sites of synapsis. First, in an analysis of the "earliest" SISs (i.e., a subset of the total limited to the shortest synaptic tracts comprising <25% of the SC), pericentromeric SISs constituted a sizable proportion: For chromosome 1, 20.0% of SISs fell into either the p- or q-arm centromeric bin (Figure 4B), for chromosome 16 the proportion was 24.0% (Figure 4B), and for chromosome 21 the value was 31.8% (Figure S2B). Second, for two of the three chromosomes examined, a difference in the extent of synapsis was evident between pericentromeric and non-centromeric SISs. Specifically, the lengths (in microns) of pericentromeric SISs were significantly longer than the tracts found on the p and q arms for chromosome 16 (mean pericentromeric SIS length = 5.82 ± 0.42 and interstitial SIS length = 2.54 ± 0.13; t = 9.50, $p < 0.0001$; Figure 4A) and for chromosome 21 (pericentromeric SIS length = 2.87 ± 0.18 and interstitial SIS length = 1.56 ± 0.14; t = 6.02, $p < 0.0001$; Figure S2A), although not for chromosome 1 (pericentromeric SIS length ± SE = 4.06 ± 0.44 and interstitial SIS length = 4.07 ± 0.18; t = 0.04, p = 0.97; Figure 4A). Assuming that the rate of spreading is similar between pericentromeric and non-centromeric SIS tracts, this suggests that, at least for some chromosomes, regions in the vicinity of the centromere are the first to synapse. Alternatively, synapsis might proceed more rapidly in pericentromeric regions, possibly due to the presence of highly repetitive sequences; in this regard, it is important to note that chromosomes 1 and 16 contain large blocks of pericentromeric heterochromatin and might not be representative of all

Table 2. Number of SISs and MLH1 Foci per Chromosome in Human Spermatocytes and Oocytes

	1	2	3	4	5	6	7	8+
Number of SISs per Chromosome (%)								
Male								
Chrom. 1	4 (3.9)	98 (96.1)	–	–	–	–	–	–
Chrom. 16	1 (1.6)	62 (98.4)	–	–	–	–	–	–
Female								
Chrom. 1	4 (3.3)	13 (10.7)	5 (4.1)	13 (10.7)	23 (18.9)	17 (13.9)	23 (18.9)	24 (19.7)
Chrom. 16	42 (21.0)	79 (39.5)	53 (26.5)	21 (10.5)	3 (1.5)	2 (1.0)	–	–
Chrom. 21	55 (40.7)	67 (45.6)	12 (8.9)	1 (0.7)	–	–	–	–
Number of MLH1 Foci per Chromosome (%)								
Male								
Chrom. 1	–	2 (1.9)	42 (40.2)	59 (56.7)	1 (1.0)	–	–	–
Chrom. 16	3 (2.8)	103 (96.3)	1 (0.9)	–	–	–	–	–
Female								
Chrom. 1	–	1 (1.3)	4 (5.2)	24 (31.2)	22 (28.6)	20 (26.0)	3 (3.9)	3 (3.9)
Chrom. 16	9 (4.2)	74 (34.1)	85 (39.2)	43 (19.8)	5 (2.3)	1 (0.5)	–	–
Chrom. 21	79 (64.8)	42 (34.4)	1 (0.8)	–	–	–	–	–

human chromosomes. In any event, the presence of these proximal SIS tracts is in sharp contrast to the human male (Figure 2A) and provides evidence for a major sex-specific difference in the synaptic behavior of pericentromeric regions—i.e., they appear to act as barriers to synapsis in the male but frequently as "hot" spots for synaptic initiation in the female.

Variation in Synaptic Patterns between Humans and Mice

To determine whether the sex-specific differences observed in humans extend to other mammalian species, we analyzed male and female mice. We used the same strategy, examining the number and location of SISs on representative large, medium, and small chromosomes: 1, 11 and 19, respectively. Because all mouse chromosomes are effectively acrocentric, only one arm per chromosome was analyzed. To minimize individual variation, we restricted our analysis to the inbred C57BL/6 strain, examining a total of 348 zygotene spermatocytes from four adult males and 335 zygotene oocytes from seven embryonic day 16 (E16) females (see Figures 5A and 5B for representative images).

In contrast to the human male, multiple SISs were common on larger chromosomes in the male mouse, and we observed a maximum number per chromosome of five, four, and two SISs for chromosomes 1, 11, and 19, respectively (Figure 5A; Table 3). The mean number of SISs was virtually identical for chromosomes 1 and 11 (2.10 ± 0.08 and 2.20 ± 0.06, respectively) but was reduced for the smallest autosome, chromosome 19 (1.26 ± 0.06).

As in the human, we divided the chromosome arms into five equal segments and assessed the placement of SIS midpoints on each chromosome, restricting our analysis to SISs that comprised less than 25% of the total SC length (Figure 5C). We observed significant variation among chromosomes with respect to the location of the SISs (i.e., $\chi^2 = 23.17$; $p = 0.003$), and two of the three pairwise comparisons were also significant (i.e., 1 versus 11, $\chi^2 = 15.31$, $p = 0.004$; 1 versus 19, $\chi^2 = 13.00$, $p = 0.011$). However, some features were shared among chromosomes. For example, no SIS "cold" spots were evident on any chromosome. Indeed, with the exception of the centromeric region on chromosome 19 (where only 4% of the total SISs for that chromosome were localized), each interval contained at least 10% of the total SISs. Each chromosome also exhibited the same preferential location; i.e., for each, the telomeric segment was the most likely to contain an SIS, with 30% or more of the SISs localizing to this region.

The mouse female, like the mouse male, frequently had multiple sites of SC initiation (Figure 5B; Table 3). The average number of SISs was only slightly higher in females, with means of 2.51 ± 0.08, 2.17 ± 0.08, and 1.62 ± 0.08 for chromosomes 1, 11, and 19, respectively; more than one-third of chromosomes 1 and 11 exhibited three or more SISs (Table 3). The chromosomal locations of SISs are summarized in Figure 5C and, as in males, there were obvious chromosome-specific effects: we observed highly significant variation among chromosomes in the proportion of SISs in the five intervals ($\chi^2 = 57.86$; $p < 0.0001$), and for two of the three pairwise comparisons, the differences were also significant (1

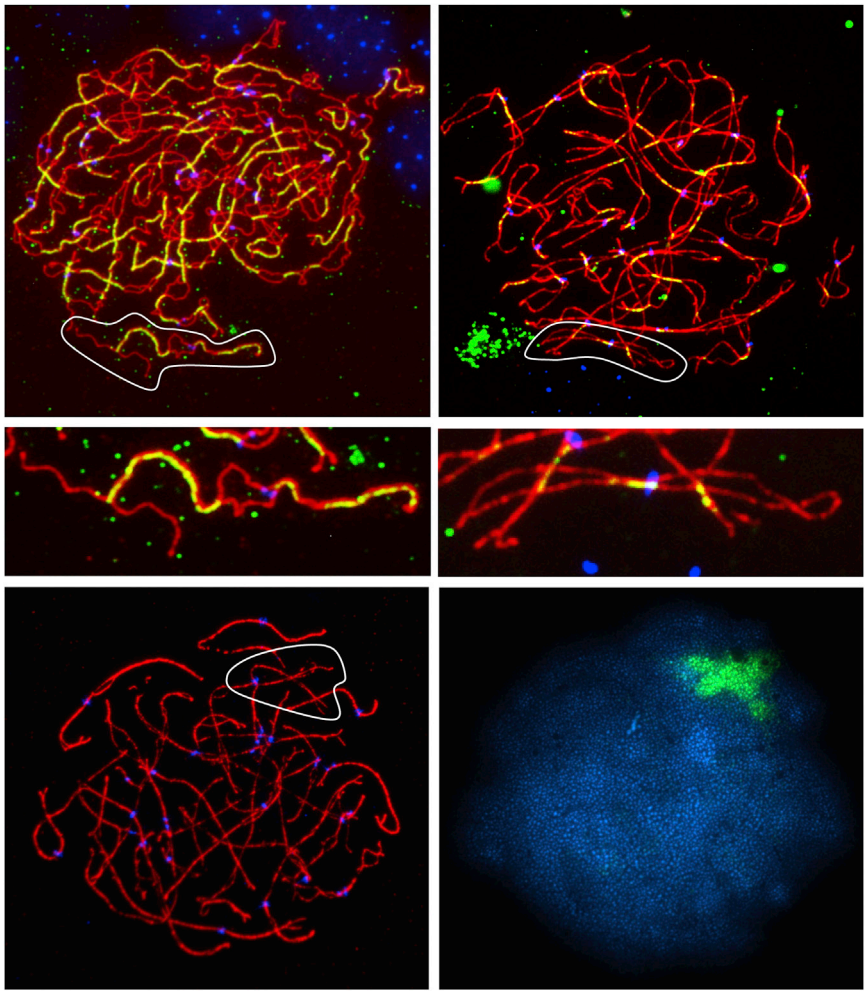

Figure 3. In Human Females, Synapsis Typically Initiates at, or near, the Centromere

Top: Examples of two zygotene-stage oocytes immunostained for the axial element protein SYCP3 (red), the transverse filament protein SYCP1 (green), and centromere-associated CREST (blue). Synapsed chromosome regions are detected by the presence of SYCP1 signals.

Middle: Magnification of the circled partially synapsed chromosome pairs from the above images, showing characteristic multiple SISs (left) and a pericentromeric SIS (right).

Bottom: Use of a chromosome paint FISH probe to identify individual chromosomes in zygotene-stage cells. On left, oocyte has been immunostained for the axial element protein SYCP3 (red) and centromere-associated CREST (blue). Circled chromosome is chromosome 16, as determined by using a paint probe; i.e., right image shows same cell, stained with DAPI and probed with a chromosome 16 paint probe (green).

versus 19, $\chi^2 = 50.88$, $p < 0.0001$; 11 versus 19, $\chi^2 = 39.38$; $p < 0.0001$). As in males, however, there were also common features: SISs occurred in all five intervals, the centromeric region of chromosome 19 being the only cold spot with limited SIS localization of 1.2%. The telomeric interval was the most likely to contain an SIS: 29.9%, 31.0%, and 55.8% for chromosomes 1, 11, and 19, respectively (Figure 5C). Thus, our observations suggest major species-specific differences in SIS placement between mice and humans and, in particular, the absence of the major sex-specific differences that characterized synapsis in humans.

SISs and Sites of Recombination in Mammals

Studies in yeast and other eukaryotic models suggest a direct link between sites of synaptic initiation and recombination.[23–26] To test this association in mammals, we compared the locations of SISs and MLH1 foci in both sexes in humans and mice. Whenever possible, comparisons were based on preparations from the same individual (i.e., scoring SISs in zygotene cells and MLH1 in pachytene cells); however, this was not possible in the female mouse, because preparations of a single gestational age typically do not contain sufficient numbers of both early zygotene and pachytene cells. The data were analyzed by two different approaches. First, we compared the localization of SISs and MLH1 foci within an individual for human males (Figure S4), human females (Figure S4), and mouse males (Figure S5). Because this was not possible in female mice, we analyzed SISs in one set of cases, and MLH1 foci in a second set (Figure S5). Second, we pooled data from individual cases and, as in our analysis of SISs, divided chromosome arms into five equal segments, comparing the location of SISs in zygotene-stage cells and of MLH1 foci in pachytene meiocytes (Figure 6).

In human males, there were important differences between the number and location of SISs and MLH1 foci. Notably, the number of MLH1 foci per chromosome often exceeded the number of SISs. That is, although we never observed more than two SISs per chromosome, the number of MLH1 foci ranged from two to five for chromosome 1 and from one to three for chromosome 16 (Table 2); accordingly, the difference in the number of SISs versus MLH1 foci per SC was highly significant for chromosome 1 ($\chi^2 = 198.84$; $p < 0.0001$), although not for chromosome 16 ($\chi^2 = 0.86$; $p = 0.65$). Further, the distribution of SISs and MLH1 foci locations was also highly significantly different (for chromosome 1, $\chi^2 = 108.53$, $p < 0.0001$; for chromosome 16, $\chi^2 = 36.53$, $p < 0.0001$; Figures 6A and S4). SISs were restricted to the distal chromosome arms (Figure 6) and although they appeared to overlap a sub-set of MLH1 foci, the latter were also observed in the three most proximal regions of each chromosome arm (Figure S4).

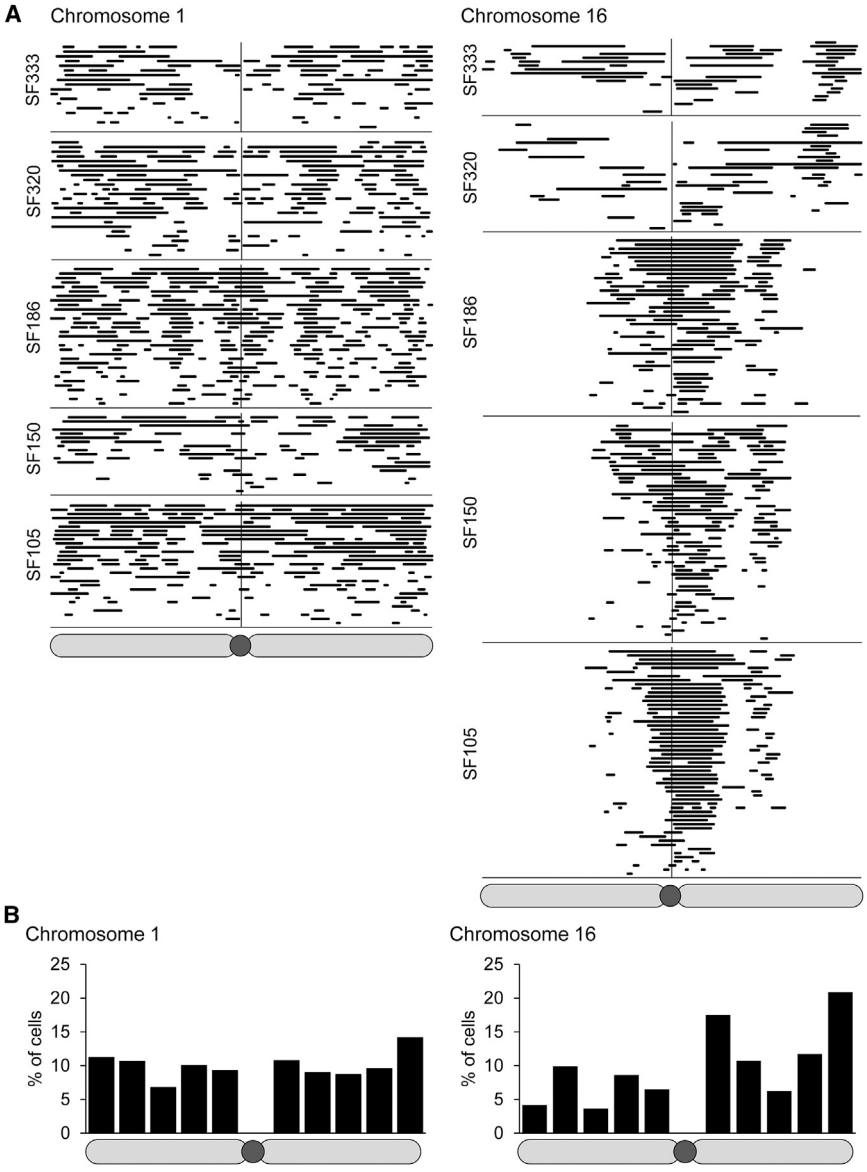

Figure 4. Chromosomal Locations of SISs in Human Females

(A) Chromosomal locations of SISs on individual chromosomes 1 or 16 from five fetal ovarian samples (SF105, SF150, SF186, SF320, and SF333); comparable data on chromosome 21 are provided in Figure S2. Each row shows the approximate length and location (as a percent of SC length) of SIS tracts on partially synapsed homologs; in total, we examined 122 partially synapsed chromosomes 1 and 200 partially synapsed chromosomes 16.

(B) A subset of data (SISs with lengths less than 25% of the chromosome length) from the five samples, showing the proportion of SISs in each chromosome region (i.e., centromeric, proximal, interstitial, distal, or telomeric) on chromosomes 1 and 16. For this analysis, the location of the SIS was taken as the midpoint of the SYCP1 signal.

In human females as in males, the numbers of MLH1 foci and SISs per chromosome were significantly different. For chromosomes 1 ($\chi^2 = 42.31$, $p < 0.0001$) and 21 ($\chi^2 = 14.71$, $p < 0.001$), there were significantly more SISs than MLH1 foci, whereas for chromosome 16 ($\chi^2 = 30.47$, $p < 0.0001$), the reverse was true (Table 2). The locations of SISs and MLH1 foci were also significantly different (for chromosome 1, $\chi^2 = 24.33$ $p < 0.005$; for chromosome 16, $\chi^2 = 62.54$, $p < 0.0001$; for chromosome 21, $\chi^2 = 49.75$, $p < 0.0001$; Figures 6A, S2, and S4) and, for each chromosome, the difference was largely attributable to the presence of SISs—but not MLH1 foci—in the pericentromeric region.

In mice, the relationship between the numbers of SISs and MLH1 foci was consistent among chromosomes and between sexes; i.e., for each chromosome there were significantly more SISs than MLH1 foci in both males (chromosome 1: $\chi^2 = 116.78$, $p < 0.0001$; 11: $\chi^2 = 121.67$, $p < 0.0001$; 19: $\chi^2 = 56.56$, $p < 0.0001$) and females (chromosome 1: $\chi^2 = 135.34$, $p < 0.0001$; 11: $\chi^2 = 133.86$, $p < 0.0001$; 19: $\chi^2 = 67.74$, $p < 0.0001$; Table 3). The location of SISs and MLH1 foci was also different from that observed in humans, with no obvious hot or cold spots for SISs or MLH1 foci in mice of either sex. Consequently, the differences in the location of SISs versus MLH1 foci were relatively subtle (Figures 6B and S5). In the male, the differences reached statistical significance for one of the three chromosomes examined (i.e., 1: $\chi^2 = 4.15$, $p = 0.39$; 11: $\chi^2 = 37.84$, $p < 0.0001$; 19: $\chi^2 = 8.26$, $p = 0.08$; Figure 6B) and, in the female, for all three chromosomes (i.e., 1: $\chi^2 = 19.07$, $p < 0.001$; 11: $\chi^2 = 27.87$, $p < 0.0001$; 19: $\chi^2 = 33.51$, $p < 0.0001$; Figure 6B). Thus, in mice as in humans, we did not observe a simple 1:1 correlation between SISs and MLH1 foci.

Discussion

The goals of this study were to determine whether homolog synapsis occurs in a similar fashion in human males and females, to compare synaptic patterns in different mammalian species, and to assess the possibility that crossovers (CO) co-localize with sites of synaptic initiation (SIS) in mammals. Our observations provide evidence for surprising variation in synaptic initiation between two mammalian species but also of remarkably different sex-specific patterns in humans. Further, the combined data from our studies in mice and humans suggest that the

Table 3. Number of SISs and MLH1 Foci per Chromosome in Mouse Spermatocytes and Oocytes

	1	2	3	4	5	6
Number (%) of SISs per Chromosome						
Male						
Chrom. 1	60 (34.5)	57 (32.8)	40 (23.0)	13 (7.5)	4 (2.3)	–
Chrom. 11	49 (23.8)	88 (42.7)	48 (23.3)	21 (10.2)	–	–
Chrom. 19	40 (74.1)	14 (26.0)	–	–	–	–
Female						
Chrom. 1	41 (20.3)	72 (35.6)	48 (23.8)	29 (14,4)	9 (4.5)	3 (1.5)
Chrom. 11	62 (33.9)	54 (29.5)	44 (24.0)	19 (10.4)	4 (2.2)	–
Chrom. 19	30 (45.5)	32 (48.5)	3 (4.5)	1 (1.5)	–	–
Number (%) of MLH1 Foci per Chromosome						
Male						
Chrom. 1	133 (43.0)	176 (57.0)	–	–	–	–
Chrom. 11	159 (50.8)	152 (48.6)	2 (0.6)	–	–	–
Chrom. 19	228 (99.6)	1 (0.4)	–	–	–	–
Female						
Chrom. 1	115 (33.6)	212 (62.0)	15 (4.4)	–	–	–
Chrom. 11	214 (63.3)	121 (35.8)	3 (0.9)	–	–	–
Chrom. 19	177 (91.7)	16 (8.3)	–	–	–	–

relationship between SISs and COs in mammals is a complex one that is not dictated by the sites of synaptic initiation as reported in other organisms, but is clearly influenced by them.

Synapsis in Mammals: Patterns Are Species Specific

Previous studies by us and others[22,27] suggested tight regulation of the initiation and progression of synapsis in human males, with a single origin of synapsis at the subtelomeric region of each chromosome arm. Limited data from a recent examination of meiotic centromeres in the mouse suggested a markedly different pattern in the male mouse, including chromosomes with multiple sites of synaptic initiation.[28] Thus, to determine the extent of these apparent species differences, we conducted a systematic examination of the onset of synapsis in males of both species.

As in our initial study of human males,[22] we found that the synaptic pattern throughout the genome was a virtual constant: we never observed more than a single SIS per chromosome arm, the centromere was never involved, and we found little evidence for either inter-individual or chromosome-specific variation. Thus, in the human male, there appears to be a "one fits all" synaptic strategy that applies to all chromosomes and chromosome arms.

Unlike humans, where most chromosomes have two arms, all mouse chromosomes are acrocentric. Nevertheless, in contrast to the pattern of a single SIS per chromosome arm observed in human males, multiple SISs were observed on all chromosomes in the male mouse, including the smallest autosome, chromosome 19. Moreover, as many as five SISs were observed on the largest chromosome, chromosome 1. Thus, with respect to synaptic initiation patterns, male mice and humans exhibit remarkable differences.

Synapsis in Males and Females: More Evidence that Men Are from Mars and Women from Venus

Early electron microscopic analyses of serially sectioned human meiocytes provided evidence of sex-specific differences in synapsis, with interstitial sites being restricted to females[29,30] (reviewed in Pfeifer et al.[31]). However, these and subsequent analyses of surface spread preparations[32–34] were based on limited numbers of cells and were not designed to uncover sex-specific differences in synapsis. Thus, to our knowledge, the present study represents the first attempt to map synaptic initiation sites in males and females and compare chromosome-specific patterns between the sexes.

Perhaps the most intriguing finding from our studies is the remarkable sex-specific difference in synaptic patterns in humans. In sharp constant to the simple strategy of a single distal synaptic site per chromosome arm in the human male, synapsis in the human female can best be described as a multitasking approach; i.e., we observed multiple SISs per chromosome for each of the three chromosomes (1, 16, and 21) examined in human females. Not only did these sites rarely involve the distal

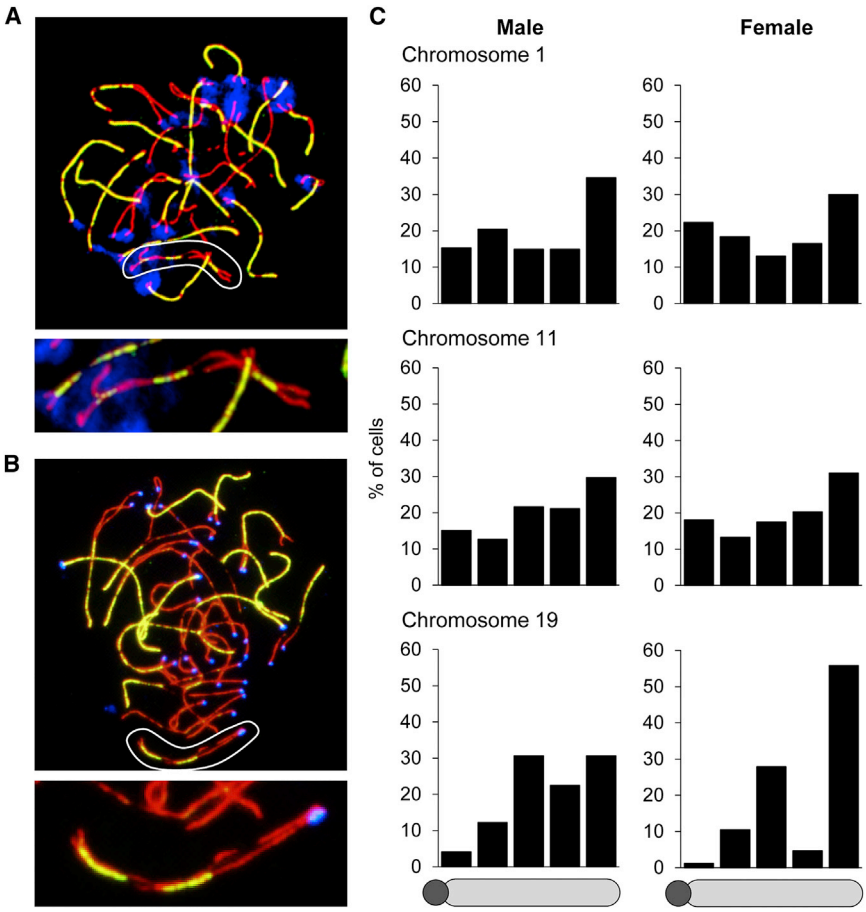

Figure 5. In Mice, Males and Females Have Similar Patterns of Synaptic Initiation

(A) Top: Example of a zygotene-stage spermatocyte immunostained for the axial element protein SYCP3 (red), the transverse filament protein SYCP1 (green), and DAPI (blue). Synapsed chromosome regions are detected by the presence of SYCP1 signals. Bottom: Enlargement of the circled partially synapsed chromosome pair from the image above, showing three SISs.

(B) Top: Example of a zygotene-stage oocyte immunostained for SYCP3 (red), SYCP1 (green), and centromere-associated CREST (blue). Bottom: Magnification of the circled partially synapsed chromosome pair from the image above, showing characteristic interstitial and distal SISs.

(C) A subset of data (SISs with lengths less than 25% of the chromosome length) from individual spermatocytes and oocytes, showing the proportion (in percentage) of SISs within different chromosome regions (centromeric, proximal, interstitial, distal, and telomeric) on chromosomes 1, 11, and 19. Note that, unlike human males or females, the distribution of SISs across the chromosome arm is relatively flat, regardless of chromosome or of sex.

regions favored in the human male, but the centromere—which acts as a synaptic barrier in the male—was the region most likely to be involved in SISs in the female. Indeed, most SCs analyzed exhibited at least one pericentromeric SIS (Figure 4A). Further, unlike the male, the number of SISs per chromosome varied widely but, in general, was correlated with chromosome size; i.e., the mean number of SISs per chromosome was 4.5 for chromosome 1, 2.3 for chromosome 16, and 1.7 for chromosome 21. Taken together, these observations provide compelling evidence that human males and females follow different—and almost diametrically opposed—rules with respect to the way in which homologs find and associate with one another in meiotic prophase.

The basis of these differences is unknown, but might reflect male:female differences in epigenetic programming. In mammalian females, meiotic prophase occurs in the fetal ovary, at a time when the genome is hypomethylated, whereas in males meiosis is not initiated until puberty, by which time the germ cell genome is highly methylated (reviewed in Kota and Feil[35]). Consequently, it might be expected that chromatin conformation would exhibit sex-specific variation and indeed, in previous comparisons of human spermatocytes and oocytes, we noted just such differences;[6] i.e., SCs were longer and DNA loops smaller in oocytes, a configuration that has been linked to increases in genome-wide recombination levels[36] and, presumably, also maximizes the likelihood of multiple points of synapsis between homologs. However, in those studies we made no attempt to examine chromatin compaction in specific chromosome regions; thus we do not know whether the sex-specific differences in SC length/DNA loop volume that we observed are dependent on chromosomal context. In light of the observations on synapsis in the present report, it seems possible that, in spermatocytes, SCs are less condensed in telomeric regions than in pericentromeric regions and that the opposite situation applies to human oocytes. Studies are presently underway to test this possibility, and thereby to determine whether differential compaction contributes to the sex-specific variation in utilization of chromosome elements in synapsis in humans.

Clearly, our data on mice present a caveat to the above argument. Although similar sex-specific differences in the epigenome are observed in both humans and rodents (reviewed in Kota and Feil[35]), our analyses provided little evidence of differences in synapsis between oocytes and spermatocytes from inbred C57BL/6 mice. Indeed, the synaptic patterns we observed in mice resemble neither the human female nor male pattern but provides a third, and seemingly intermediate, pattern: multiple SISs were evident in both male and female mice, although the

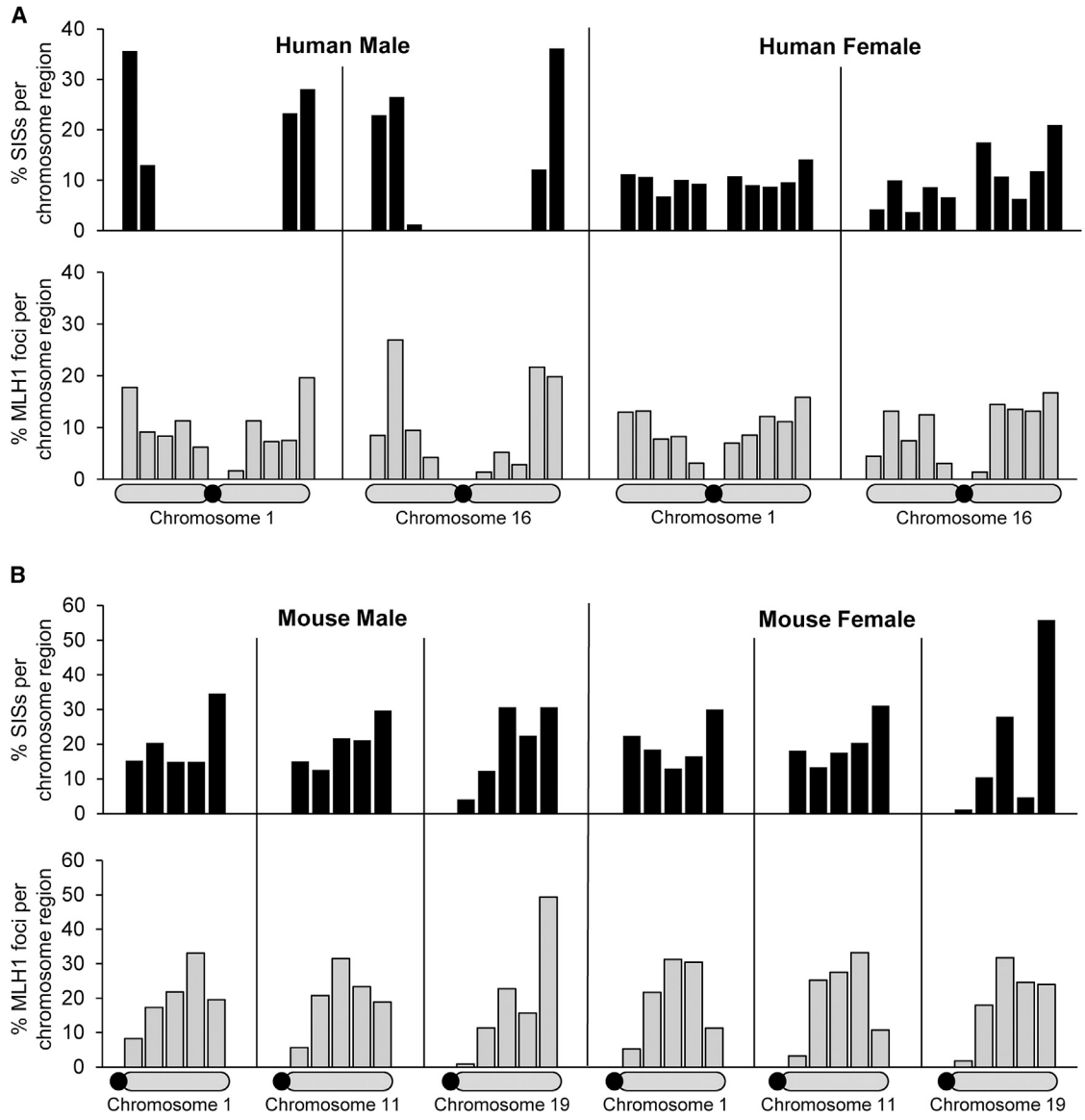

Figure 6. Comparison of Patterns of Localization of SISs and MLH1 Foci in Humans and Mice

(A) Left: A subset of zygotene-stage data (i.e., SISs with lengths less than 25% of the chromosome length) and pachytene data on MLH1 localization from three males (OA32, OA34, and OA36), pooled to show the proportion of SISs and MLH1 foci in different regions of the p and q arms of chromosomes 1 and 16. The distributions of SISs and MLH1 foci were significantly different for both chromosomes 1 and 16 (1: $\chi^2 = 108.53$, $p < 0.0001$; 16: $\chi^2 = 36.25$, $p < 0.0001$). Right: A dataset similar to that for males from human females SF105, SF320, and SF333; SIS and MLH1 placements were significantly different for both chromosomes 1 and 16 (1: $\chi^2 = 24.33$, $p < 0.005$; 16: $\chi^2 = 62.54$, $p < 0.0001$).

(B) Left: A subset of zygotene-stage data (SISs with lengths less than 25% of the chromosome length) and pachytene data from four adult male mice (B6, 886, 1238, and 1474), showing the proportion of SISs and MLH1 foci in different chromosome regions. Distributions of SISs and MLH1 foci were significantly different for chromosome 11 (11: $\chi^2 = 37.84$, $p < 0.0001$) but not for chromosome 1 or 19 (1: $\chi^2 = 4.15$; $p = 0.39$; 19: $\chi^2 = 8.26$; $p = 0.08$). Right: A dataset similar to that for males but with information on SISs from seven E16 female mice (1029.6, 1029.9, 1049.4, 1087.3, 1084.5, 1324.4, and 1324.7) and on MLH1 foci from five E18.5 female mice (1230.2, 1230.8, 1236.1, 1236.2, and 1275.2). Placement of SISs and MLH1 foci were significantly different for all three chromosomes (1: $\chi^2 = 19.07$; $p < 0.001$; 11: $\chi^2 = 27.87$; $p < 0.0001$; 19: $\chi^2 = 33.51$; $p < 0.0001$).

average number was slightly higher in females (i.e., with female:male ratios of 2.1 to 1, 1 to 1, and 1.3 to 1 for chromosomes 1, 11, and 19, respectively). Further, although there was slight variation among chromosomes, sites of synaptic initiation were observed in all intervals and the distribution along the arm was relatively flat in both sexes (Figure 5C).

Synapsis and Crossovers Are Correlated, but There Is Not a 1:1 Relationship in Mice or Humans

Studies in a variety of organisms indicate a relationship—if not an exact match—between sites of SC initiation and the occurrence of crossovers (for reviews, see Henderson and Keeney[17] and Zickler[18]). For example, early cytological studies in maize, Sordaria, and Neurospora, among other

species, suggested a correlation between SC initiation sites and recombination nodules.[24–26] More recently, molecular analyses of SC proteins in yeast have provided additional evidence of an association. First, immunofluorescence analysis of the synaptic initiation complex-associated protein Zip2 at zygotene indicate that, like crossovers, Zip2 foci display interference.[37] Second, mutations in the DSB-inducing protein Spo11 disturb the localization pattern of another synaptic initiation complex-associated protein, Zip3.[38] Lastly, mutations in components of the synaptic initiation complex interfere with the processing of recombination intermediates.[39]

Thus, we were interested in asking whether SIS and MLH1 focus localization patterns are correlated in mammals. Superficially, the answer appears to be no, for three reasons. First, in human males, MLH1 foci were often located in chromosome regions that were devoid of SISs (Figure 6A). Specifically, for chromosome 1, 46% of MLH1 foci localized to the proximal three-fifths of the chromosome arms, and for chromosome 16 the value was 23%; in contrast, only a single SIS (out of 325) mapped to these regions. Second, the opposite situation applied to human oocytes; i.e., on each of the three chromosomes analyzed, we observed a preponderance of pericentromeric SISs, despite the fact that MLH1 foci rarely localized to these regions (Figures 6A and S2). This is reminiscent of observations in *S. cerevisiae*, in which centromeric regions are thought to be preferred sites of synaptic initiation, although—unlike sites of synapsis in non-centromeric regions—they are not translated into crossovers.[40] Similarly, our observations on the length of SYCP1 tracts in human oocytes suggest that pericentromeric SISs are early forming, but do not lead to crossover events. Third, our data from synaptic studies in mice also failed to provide evidence for a 1:1 correlation between SISs and MLH1 foci since, in both sexes, the number of SISs exceeded the number of MLH1 foci for each of the three chromosomes analyzed. Thus, the weight of evidence from both humans and mice suggests that the sites of SISs and crossovers are not directly correlated.

Against this background, however, several lines of evidence suggest that a subset of SISs and MLH1 foci might indeed be linked to one another. First, the number and overall pattern of SIS localization in humans mirror results of human linkage and cytological analyses.[11–15] That is, linkage studies indicate that human females have approximately 1.6-fold the number of crossovers as males and in this study we observed a similar excess of SISs in females (with female/male ratios of 2.9 to 1 and 1.2 to 1 for chromosomes 1 and 16, respectively). Second, these observations are echoed by similar data from mice: previous cytological studies of recombination in inbred strains suggest subtle, but significant, sex-specific differences in genome-wide recombination levels (assessed by the number of MLH1 foci per cell), with females typically having higher rates than males.[36,41] Consistent with this, we observed a slight female excess of SISs on chromosomes 1 and 19, although values were similar in males and females on chromosome 11. Finally, a comparison of the distribution of MLH1 foci and SISs (Figures 6 and S2) indicates considerable overlap in chromosomal location in both species and in both sexes. That is, in human males most SISs and MLH1 foci were sub-telomeric in location, whereas in human females and in mice both SISs and MLH1 foci were relatively evenly distributed along the chromosome arms.

Taken together, our data suggest that, in humans and in mice, sites of synaptic initiation are not directly converted into crossovers as reported in some species, but that the two processes are correlated. That is, either a subset of SISs and crossovers occur at the same sites or there is a more general relationship, possibly associated with similarities in the generation of SISs and crossover precursors. In this regard, recent studies of recombination hotspots by Pratto et al.[42] might be relevant. They reported a temporal change in the chromosomal localization of the meiosis-specific DSB-associated protein DMC1 in prophase-stage human spermatocytes; specifically, DMC1 foci were found clustered close to the telomeres in early zygotene spermatocytes but were more interstitially positioned in late zygotene cells. Potentially, the initial wave of DSBs form in conjunction with SISs, and a smaller proportion of later forming, interstitially placed DBSs are not dependent on the presence of SISs. This is consistent with our observations and would provide an explanation for the co-localization of some, but not all, SISs and MLH1 foci in human spermatocytes. Further, the same general relationship between SISs and DSBs might also apply in human females, but with DSBs being excluded from highly repetitive chromosome segments (e.g., pericentromeric regions). Accordingly, DSBs would be preferentially located within the interstitial regions, thus matching the observed non-centromeric SIS and CO distributions in human oocytes.

The variation that we observed between humans and mice and the lack of a major sex-specific difference in the distributions of SISs and MLH1 foci in mice remains to be explained. Clearly, a useful short-term goal would be an examination of non-human primates, to determine whether the male:female differences we identified in humans extend to other closely related species. More generally, an important challenge to our understanding of mammalian recombination will be determining the molecular mechanisms by which SISs influence crossovers and how these mechanisms differ among various species.

Supplemental Data

Supplemental Data include five figures and can be found with this article online at http://dx.doi.org/10.1016/j.ajhg.2015.11.019.

Acknowledgments

We thank the staff and faculty at San Francisco General Hospital's Women's Options Center for assistance in the collection of tissues.

We also thank Tracey Woodruff, Victor Fujimoto, Carrie Dickenson, Cheryl Godwin De Medina, Katie Stevenson, Dylan Atchley, Cynthia Megloza, Jody Steinauer, Janet Pan, Changqing Zhou, and Crystal Lawson for their assistance in recruitment, data collection, and manuscript preparation. This work was supported by NIH grants R37 HD21341 (to T.H.) and R01 ES13527 (to P.A.H.).

Received: October 12, 2015
Accepted: November 16, 2015
Published: December 31, 2015

Web Resources

The URL for data presented herein is as follows:

OMIM, http://www.omim.org/

References

1. Hassold, T., and Hunt, P. (2001). To err (meiotically) is human: the genesis of human aneuploidy. Nat. Rev. Genet. *2*, 280–291.
2. Lamb, N.E., Freeman, S.B., Savage-Austin, A., Pettay, D., Taft, L., Hersey, J., Gu, Y., Shen, J., Saker, D., May, K.M., et al. (1996). Susceptible chiasmate configurations of chromosome 21 predispose to non-disjunction in both maternal meiosis I and meiosis II. Nat. Genet. *14*, 400–405.
3. Lamb, N.E., Sherman, S.L., and Hassold, T.J. (2005). Effect of meiotic recombination on the production of aneuploid gametes in humans. Cytogenet. Genome Res. *111*, 250–255.
4. Oliver, T.R., Feingold, E., Yu, K., Cheung, V., Tinker, S., Yadav-Shah, M., Masse, N., and Sherman, S.L. (2008). New insights into human nondisjunction of chromosome 21 in oocytes. PLoS Genet. *4*, e1000033.
5. Cheng, E.Y., Hunt, P.A., Naluai-Cecchini, T.A., Fligner, C.L., Fujimoto, V.Y., Pasternack, T.L., Schwartz, J.M., Steinauer, J.E., Woodruff, T.J., Cherry, S.M., et al. (2009). Meiotic recombination in human oocytes. PLoS Genet. *5*, e1000661.
6. Gruhn, J.R., Rubio, C., Broman, K.W., Hunt, P.A., and Hassold, T. (2013). Cytological studies of human meiosis: sex-specific differences in recombination originate at, or prior to, establishment of double-strand breaks. PLoS ONE *8*, e85075.
7. Tease, C., Hartshorne, G.M., and Hultén, M.A. (2002). Patterns of meiotic recombination in human fetal oocytes. Am. J. Hum. Genet. *70*, 1469–1479.
8. Kong, A., Thorleifsson, G., Frigge, M.L., Masson, G., Gudbjartsson, D.F., Villemoes, R., Magnusdottir, E., Olafsdottir, S.B., Thorsteinsdottir, U., and Stefansson, K. (2014). Common and low-frequency variants associated with genome-wide recombination rate. Nat. Genet. *46*, 11–16.
9. Baier, B., Hunt, P., Broman, K.W., and Hassold, T. (2014). Variation in genome-wide levels of meiotic recombination is established at the onset of prophase in mammalian males. PLoS Genet. *10*, e1004125.
10. Lynn, A., Ashley, T., and Hassold, T. (2004). Variation in human meiotic recombination. Annu. Rev. Genomics Hum. Genet. *5*, 317–349.
11. Broman, K.W., Murray, J.C., Sheffield, V.C., White, R.L., and Weber, J.L. (1998). Comprehensive human genetic maps: individual and sex-specific variation in recombination. Am. J. Hum. Genet. *63*, 861–869.
12. Kong, A., Gudbjartsson, D.F., Sainz, J., Jonsdottir, G.M., Gudjonsson, S.A., Richardsson, B., Sigurdardottir, S., Barnard, J., Hallbeck, B., Masson, G., et al. (2002). A high-resolution recombination map of the human genome. Nat. Genet. *31*, 241–247.
13. Matise, T.C., Chen, F., Chen, W., De La Vega, F.M., Hansen, M., He, C., Hyland, F.C.L., Kennedy, G.C., Kong, X., Murray, S.S., et al. (2007). A second-generation combined linkage physical map of the human genome. Genome Res. *17*, 1783–1786.
14. Jorgenson, E., Tang, H., Gadde, M., Province, M., Leppert, M., Kardia, S., Schork, N., Cooper, R., Rao, D.C., Boerwinkle, E., and Risch, N. (2005). Ethnicity and human genetic linkage maps. Am. J. Hum. Genet. *76*, 276–290.
15. Ju, Y.S., Park, H., Lee, M.K., Kim, J.-I., Sung, J., Cho, S.-I., and Seo, J.-S. (2008). A genome-wide Asian genetic map and ethnic comparison: the GENDISCAN study. BMC Genomics *9*, 554.
16. Kleckner, N., Storlazzi, A., and Zickler, D. (2003). Coordinate variation in meiotic pachytene SC length and total crossover/chiasma frequency under conditions of constant DNA length. Trends Genet. *19*, 623–628.
17. Henderson, K.A., and Keeney, S. (2005). Synaptonemal complex formation: where does it start? BioEssays *27*, 995–998.
18. Zickler, D. (2006). From early homologue recognition to synaptonemal complex formation. Chromosoma *115*, 158–174.
19. Peters, A.H., Plug, A.W., van Vugt, M.J., and de Boer, P. (1997). A drying-down technique for the spreading of mammalian meiocytes from the male and female germline. Chromosome Res. *5*, 66–68.
20. Topping, D., Brown, P., Judis, L., Schwartz, S., Seftel, A., Thomas, A., and Hassold, T. (2006). Synaptic defects at meiosis I and non-obstructive azoospermia. Hum. Reprod. *21*, 3171–3177.
21. Reeves, A., and Tear, J. (2000). MicroMeasure for Windows, version 3.3.
22. Brown, P.W., Judis, L., Chan, E.R., Schwartz, S., Seftel, A., Thomas, A., and Hassold, T.J. (2005). Meiotic synapsis proceeds from a limited number of subtelomeric sites in the human male. Am. J. Hum. Genet. *77*, 556–566.
23. Agarwal, S., and Roeder, G.S. (2000). Zip3 provides a link between recombination enzymes and synaptonemal complex proteins. Cell *102*, 245–255.
24. Zickler, D., Moreau, P.J., Huynh, A.D., and Slezec, A.M. (1992). Correlation between pairing initiation sites, recombination nodules and meiotic recombination in *Sordaria macrospora*. Genetics *132*, 135–148.
25. Maguire, M.P., and Riess, R.W. (1994). The relationship of homologous synapsis and crossing over in a maize inversion. Genetics *137*, 281–288.
26. Bojko, M. (1989). Two kinds of "recombination nodules" in *Neurospora crassa*. Genome *32*, 309–317.
27. Barlow, A.L., and Hultén, M.A. (1996). Combined immunocytogenetic and molecular cytogenetic analysis of meiosis I human spermatocytes. Chromosome Res. *4*, 562–573.
28. Bisig, C.G., Guiraldelli, M.F., Kouznetsova, A., Scherthan, H., Höög, C., Dawson, D.S., and Pezza, R.J. (2012). Synaptonemal complex components persist at centromeres and are required for homologous centromere pairing in mouse spermatocytes. PLoS Genet. *8*, e1002701.
29. Rasmussen, S., and Holm, P. (1978). Human meiosis II. chromosome pairing and recombination nodules in human spermatocytes. Carlsberg Res. Commun. *43*, 275–327.
30. Bojko, M. (1983). Human meiosis VIII. Chromosome pairing and formation of the synaptonemal complex in oocytes. Carlsberg Res. Commun. *48*, 457–483.

31. Pfeifer, C., Scherthan, H., and Thomsen, P.D. (2003). Sex-specific telomere redistribution and synapsis initiation in cattle oogenesis. Dev. Biol. *255*, 206–215.
32. Barlow, A.L., and Hultén, M.A. (1998). Crossing over analysis at pachytene in man. Eur. J. Hum. Genet. *6*, 350–358.
33. Barlow, A.L., and Hultén, M.A. (1998). Combined immunocytogenetic and molecular cytogenetic analysis of meiosis I oocytes from normal human females. Zygote *6*, 27–38.
34. Speed, R.M., and Chandley, A.C. (1990). Prophase of meiosis in human spermatocytes analysed by EM microspreading in infertile men and their controls and comparisons with human oocytes. Hum. Genet. *84*, 547–554.
35. Kota, S.K., and Feil, R. (2010). Epigenetic transitions in germ cell development and meiosis. Dev. Cell *19*, 675–686.
36. Lynn, A., Koehler, K.E., Judis, L., Chan, E.R., Cherry, J.P., Schwartz, S., Seftel, A., Hunt, P.A., and Hassold, T.J. (2002). Covariation of synaptonemal complex length and mammalian meiotic exchange rates. Science *296*, 2222–2225.
37. Fung, J.C., Rockmill, B., Odell, M., and Roeder, G.S. (2004). Imposition of crossover interference through the nonrandom distribution of synapsis initiation complexes. Cell *116*, 795–802.
38. Henderson, K.A., and Keeney, S. (2004). Tying synaptonemal complex initiation to the formation and programmed repair of DNA double-strand breaks. Proc. Natl. Acad. Sci. USA *101*, 4519–4524.
39. Börner, G.V., Kleckner, N., and Hunter, N. (2004). Crossover/noncrossover differentiation, synaptonemal complex formation, and regulatory surveillance at the leptotene/zygotene transition of meiosis. Cell *117*, 29–45.
40. Tsubouchi, T., Macqueen, A.J., and Roeder, G.S. (2008). Initiation of meiotic chromosome synapsis at centromeres in budding yeast. Genes Dev. *22*, 3217–3226.
41. Dumont, B.L., and Payseur, B.A. (2011). Genetic analysis of genome-scale recombination rate evolution in house mice. PLoS Genet. *7*, e1002116.
42. Pratto, F., Brick, K., Khil, P., Smagulova, F., Petukhova, G.V., and Camerini-Otero, R.D. (2014). DNA recombination. Recombination initiation maps of individual human genomes. Science *346*, 1256442.